NIH Public Access
Author Manuscript
J Neurochem. Author manuscript; available in PMC 2014 December 01.

Published in final edited form as:
J Neurochem. 2013 December ; 127(5): 660–668. doi:10.1111/jnc.12435.

Non-invasive detection of neurochemical changes prior to overt pathology in a mouse model of spinocerebellar ataxia type 1

Uzay E. Emir[*,1], **Howard Brent Clark**[†], **Manda L. Vollmers**[*], **Lynn E. Eberly**[‡], and **Gülin Öz**[*]

[*]Department of Radiology, Medical School, Center for Magnetic Resonance Research, University of Minnesota, Minneapolis, Minnesota, USA

[†]Department of Laboratory Medicine and Pathology, Medical School, University of Minnesota, Minneapolis, Minnesota, USA

[‡]Division of Biostatistics, School of Public Health, University of Minnesota, Minneapolis, Minnesota, USA

Abstract

Spinocerebellar ataxia type 1 (SCA1) is a hereditary, progressive and fatal movement disorder that primarily affects the cerebellum. Non-invasive imaging markers to detect early disease in SCA1 will facilitate testing and implementation of potential therapies. We have previously demonstrated the sensitivity of neurochemical levels measured by ^{1}H magnetic resonance spectroscopy (MRS) to progressive neurodegeneration using a transgenic mouse model of SCA1. In order to investigate very early neurochemical changes related to neurodegeneration, here we utilized a knock-in mouse model, the *Sca1*$^{154Q/2Q}$ line, which displays milder cerebellar pathology than the transgenic model. We measured cerebellar neurochemical profiles of *Sca1*$^{154Q/2Q}$ mice and wild-type littermates using 9.4T MRS at ages 6, 12, 24, and 39 weeks and assessed the cerebellar pathology of a subset of the mice at each time point. The *Sca1*$^{154Q/2Q}$ mice displayed very mild cerebellar pathology even at 39 weeks, however, were distinguished from wild types by MRS starting at 6 weeks. Taurine and total choline levels were significantly lower at all ages and glutamine and total creatine levels were higher starting at 12 weeks in *Sca1*$^{154Q/2Q}$ mice than controls, demonstrating the sensitivity of neurochemical levels to neurodegeneration related changes in the absence of overt pathology.

Keywords

cerebellum; histology; magnetic resonance spectroscopy; mouse model; neurodegeneration; SCA1

© 2013 International Society for Neurochemistry

Address correspondence and reprint requests to Gülin Öz, Center for MR Research, 2021 6th St. S.E., Minneapolis, MN 55455, USA. gulin@cmrr.umn.edu.
[1]Present address: Oxford Centre for Functional MRI of the Brain (FMRIB), John Radcliffe Hospital, University of Oxford, Headington, Oxford OX3 9DU, UK.

Disclosure/Conflict of interest
The authors declare no conflict of interest.

NIH-PA Author Manuscript
NIH-PA Author Manuscript
NIH-PA Author Manuscript

NIH-PA Author Manuscript

NIH-PA Author Manuscript

NIH-PA Author Manuscript

Spinocerebellar ataxias (SCAs) are a clinically and genetically heterogeneous group of autosomal dominantly inherited neurodegenerative diseases characterized by loss of cerebellar Purkinje cells (PCs) (Schöls *et al.* 2004). Six SCA subtypes, including SCA1, are caused by CAG trinucleotide repeat expansions in the respective genes, resulting in polyglutamine expansions in the expressed proteins (Zoghbi and Orr 2000). Cerebellar and, in many cases, brainstem degeneration in SCAs result in progressive loss of motor coordination and affect gaze, speech, gait and balance. As with all neurodegenerative diseases, there is a great need for biomarkers to monitor disease onset and progression directly in the brain. In particular, outcome measures that are complementary to clinical scales are needed (Klockgether 2011) to evaluate the effects of potential therapies in the brain (Klockgether and Paulson 2011). Successful implementation of such interventions will be facilitated by early detection of cerebellar abnormalities, potentially preceding clinical abnormalities.

To this end, we have previously demonstrated the sensitivity of ^{1}H magnetic resonance spectroscopy (MRS) to progressive neurodegeneration in a transgenic mouse model of SCA1 (Öz *et al.* 2010b). That model, designated as the *SCA1[82Q]* line, over-expresses the mutant human ataxin-1 protein with an 82 glutamine stretch under the control of a PC specific promoter (Burright *et al.* 1995) and displays neuronal dysfunction apparent as dendritic atrophy starting at 6 weeks. Neurodegeneration in the *SCA1[82Q]* line progresses to severe cerebellar pathology by 1 year. A subset of the neurochemicals detected by ^{1}H MRS (*N*-acetylaspartate, *myo*-inositol and glutamate) showed progressive alterations relative to control mice and significantly correlated with pathology scores in our study using the *SCA1[82Q]* mice (Öz *et al.* 2010b). Remarkably, the same neurochemicals also correlated with the ataxia score in patients (Öz *et al.* 2010a), indicating these metabolites as biomarkers of disease progression and substantiating an ability to translate the mouse findings to patients. In the *SCA1[82Q]* model, we identified another set of neurochemicals (total creatine, glutamine, and taurine) that marked the earliest biochemical changes. Namely, these metabolites were altered in the *SCA1[82Q]* mice at 6 weeks, but converged with the levels of control groups as the animals aged. In a separate study, we utilized conditional expression of the transgene in *SCA1[82Q]* mice to establish the sensitivity of MRS biomarkers to disease reversal (Öz *et al.* 2011).

While the *SCA1[82Q]* line was highly valuable to demonstrate the sensitivity of ^{1}H MRS measures to progressive neurodegeneration in SCA1, this line expresses the mutant ataxin-1 mRNA at around 50–100 times endogenous levels in PCs, therefore the disease is restricted to PCs and a cerebellar phenotype, and the mice live a normal life span. On the other hand, patients with SCA1 also develop non-cerebellar, e.g. cognitive, bulbar motor and even extrapyramidal features as the disease progresses, and die prematurely. To overcome the limitations of the transgenic SCA1 model and to guarantee accurate temporal and spatial expression patterns at endogenous levels, a knock-in mouse model of SCA1 was developed whereby the human mutation was introduced into the corresponding mouse gene (Watase *et al.* 2002): The $Sca1^{154Q/2Q}$ line has a 154 polyglutamine repeat in the endogenous ataxin-1 protein (the mouse Sca1 gene contains two CAGs at this site while the rest of the gene is highly homologous to the human SCA1 gene). These mice have learning and memory

NIH-PA Author Manuscript

NIH-PA Author Manuscript

NIH-PA Author Manuscript

deficits and suffer muscle wasting and premature death similar to human patients. In addition, PC loss occurs only at the end stage of disease and the cerebellar pathology is milder than the transgenic *SCA1[82Q]* mice. Therefore, we expanded our correlative MRS and histology work into the knock-in line to take advantage of these features of the $Sca1^{154Q/2Q}$ mice, in particular the milder cerebellar pathology. We hypothesized that metabolite levels measured by ultra-high field MRS would be sensitive to disease even prior to the development of clear pathological changes. To test this hypothesis, we compared the cerebellar neurochemical profiles of $Sca1^{154Q/2Q}$ mice longitudinally to those of wild-type (WT) littermates and assessed the cerebella of the mice at the same time points by histology.

Materials and methods

Study design

A total of 23 male mice ($Sca1^{154Q/2Q}$ knock-in mice, $n = 13$, and WT littermates, $n = 10$) were studied. Mice were obtained from 8 different litters to introduce inter-litter variability. MRS neurochemical profiles and histology data were obtained at ages 6, 12, 24, and 39 weeks. These ages were selected based on the previously characterized pathological progression in these mice (Watase *et al.* 2002). Particularly, 39 weeks was selected as the last study point since the $Sca1^{154Q/2Q}$ knock-in mice were reported to die prematurely between 35 and 45 weeks of age (Watase *et al.* 2002). Two-to-four mice were studied from each litter starting at 6 weeks of age (except for three mice that received their first scans at 12 weeks) and assigned randomly to 6, 12, 24, or 39 week follow-up. Each animal was killed for histological evaluation at its assigned time point within 24 h after MR scanning. The study was designed this way in order to have a higher number of MRS measurements at the earlier time points where neurochemical alterations were expected to be more subtle than late stage disease. This design yielded MRS data from 20 mice ($n = 11$ $Sca1^{154Q/2Q}$) at 6 weeks, from 20 mice ($n = 11$ $Sca1^{154Q/2Q}$) at 12 weeks, from 13 mice ($n = 7$ $Sca1^{154Q/2Q}$) at 24 weeks and from seven mice ($n = 4$ $Sca1^{154Q/2Q}$) at 39 weeks and also provided three to seven animals at each time point to compare the MRS and histology results in the same brains.

Animal preparation for MR scanning

All experiments were performed according to procedures approved by the University of Minnesota Institutional Animal Care and Use Committee and ARRIVE guidelines were followed in reporting. Mice were housed in mixed genotype groups, two to four per cage, in a specific pathogen free facility. Food and water were given ad libitum. Procedures for anesthesia and MR scanning were identical to our prior studies (Öz *et al.* 2010b, 2011). Briefly, mice were induced with 3–4% isoflurane prior to MR scanning and were maintained anesthetized with 1.5–2% isoflurane during scanning. Body temperature was maintained at 36–37°C and respiration rate at ~ 70–100 breaths per minute. The typical scanning time for each animal was approximately 50 min.

MR protocol

The MR scanning protocol was identical to our prior studies (Öz *et al.* 2010b, 2011). Briefly, studies were performed using a quadrature surface RF coil and a 9.4 T/31 cm

NIH-PA Author Manuscript

NIH-PA Author Manuscript

NIH-PA Author Manuscript

magnet (Magnex Scientific, Abingdon, UK) interfaced to a Varian INOVA console (Varian, Inc., Palo Alto, CA, USA). The cerebellar volume-of-interest (VOI, 5–7 μL, e.g. 1.7 × 2.1 × 1.7 mm^3 was a typical voxel size, Fig. 1a) was selected based on coronal and sagittal multi-slice images obtained with a rapid acquisition with relaxation enhancement sequence (Hennig *et al.* 1986). The VOI was positioned consistently in follow-up scans by using anatomical landmarks. Because no visually appreciable, progressive cerebellar atrophy was detected in this SCA1 model of early cerebellar disease, the VOI size was kept the same in follow-up scans of most mice. In a few mice the VOI size was reduced in one or two dimensions by 0.1 mm. All first- and second-order shims were adjusted using fast automatic shimming technique by mapping along projections (Gruetter and Tkáč 2000). Localized ^1H MR spectra were acquired with a short-echo localization by adiabatic selective refocusing sequence (TE = 15 ms, TR = 5 s, 256 averages) (Garwood and DelaBarre 2001), as described previously (Öz *et al.* 2010b). Spectra were acquired and saved as single scans, which were individually frequency and phase corrected. Scans that showed evidence for motion were excluded and the remaining scans summed. No CSF contribution was found based on unsuppressed water spectra acquired in a subset of animals at TE = 5–400 ms and TR = 30 s, and hence no correction for CSF was necessary.

Metabolite quantification

The contributions of individual metabolites to the spectra were quantified using LCModel (Provencher 1993) relative to unsuppressed water spectra acquired from the same VOI, as described before (Öz *et al.* 2010b). Reliable concentrations were selected based on Cramér-Rao lower bounds (CRLB) criteria that were identical to our prior study (Öz *et al.* 2010b). Alanine, aspartate, glycine, and *scyllo*-inositol were excluded from final analysis based on these criteria (quantification with CRLB < 50% in at least 90% of the spectra). If the correlation between two metabolites was consistently high (correlation coefficient less than −0.5), their sum was reported (Provencher 2001). Strong negative correlation was found between creatine and phosphocreatine and between glycerophosphocholine and phosphocholine, therefore, total creatine (tCr) and total choline (tCho) were reported. Based on these reliability criteria, 14 statistically uncorrelated concentrations were evaluated: ascorbate (Asc), GABA, glucose (Glc), glutamine (Gln), glutamate (Glu), glutathione (GSH), *myo*-inositol (*myo*-Ins), lactate (Lac), *N*-acetylaspartate (NAA), *N*-acetylaspartylglutamate (NAAG), phosphoethanolamine (PE), taurine (Tau), tCr, and tCho. Concentrations were not corrected for metabolite specific T_2 values (Xin *et al.* 2008), therefore the concentrations reported will be slightly over- or under-estimated relative to true concentrations in tissue in all mice. However, these effects are minimal at the short echo time (TE) of 15 ms and with the localization by adiabatic selective refocusing sequence that results in longer apparent T_2 relaxation times than those measured with conventional Hahn spin echo sequences (Michaeli *et al.* 2002).

Histology

Histology was performed in a blind fashion (regarding the group and age of the animals) following sacrifice by transcardial perfusion with pH 7.4 phosphate buffered saline and formalin (Öz *et al.* 2010b). Hematoxylin-and-eosin staining was utilized in all cases, and calbindin immunohistochemistry in some cases. The molecular layer (ML) thickness at the

NIH-PA Author Manuscript

NIH-PA Author Manuscript

NIH-PA Author Manuscript

primary fissure and a previously described severity scale (Öz *et al.* 2010b) were used to enable comparison of pathological severity in the *Sca1*$^{154Q/2Q}$ mice to our prior work in transgenic SCA1 mouse models (Öz *et al.* 2010b, 2011). In this semi-quantitative severity scale, a score of 0 designates no pathological changes and the maximum score of 4 designates severe disorganization of cerebellar cortex with generalized severe atrophy of the ML and PC loss.

Statistical analysis

For each metabolite separately, repeated measures ANOVA was used to model the effects of age, group, and their interaction on metabolite concentration. Groups were compared at each age with stepdown Bonferroni adjustment for multiple comparisons. Residual diagnostics were examined to verify that data fit model assumptions. Histology data (ML thickness and severity scores) were compared within age between groups using non-parametric Kruskal–Wallis tests because of the small sample size.

Results

All mice survived the study duration they were assigned to, namely 6, 12, 24, or 39 weeks. The WT mice continued to gain weight up to 39 weeks, while the *Sca1*$^{154Q/2Q}$ mice showed growth retardation after 6 weeks of age (Fig. 2a), as was also shown previously in this line (Watase *et al.* 2002). The molecular layer thickness at the primary fissure, a region covered by the MRS VOI (Fig. 1), did not differ between groups (Fig. 2b). The histological severity score, which takes into account pathological changes in the entire cerebellum, showed a trend to be higher by ~ 0.5 points in the *Sca1*$^{154Q/2Q}$ group vs. WT mice starting at 12 weeks and this difference became significant at end-stage (Fig. 2c). Namely, all *Sca1*$^{154Q/2Q}$ mice analyzed by histology at 39 weeks had a score of 1, while all WT mice had a score of 0.5 at this age. Note that the score of 1 (out of a maximum severity score of 4) still designates minor pathological changes largely confined to the posterior lobules of the cerebellum (Öz *et al.* 2010b), which are not covered by the MRS VOI.

High-quality MR spectra (good signal-to-noise ratio, resolution, water/lipid/artifact suppression) were obtained from the cerebella of both WT and *Sca1*$^{154Q/2Q}$ mice across their life span (Fig. 3). Of the 14 metabolites that passed our CRLB-based reliability criteria, 8 (NAA, tCr, tCho, *myo*-Ins, Glu, Gln, Tau, Lac) were quantified with mean CRLB ≤ 4%, 4 (GABA, GSH, Glc, Asc) were quantified with mean CRLB ≤ 8%, and the remaining 2 (NAAG, PE) were quantified with mean CRLB ≤ 17%.

When neurochemical profiles of the mice were compiled, 1 WT mouse and 3 *Sca1*$^{154Q/2Q}$ mice (all from different litters) were found to have an abnormal ‘high Gln’ profile that was previously described in the brains of both WT and genetically modified mice derived from the C57BL/6 strain (Tkáč *et al.* 2011; Cudalbu *et al.* 2013). The abnormal profile consisted of 2–3 fold higher Gln, 15–45% lower *myo*-Ins and 10–20% lower Tau relative to other WT or *Sca1*$^{154Q/2Q}$ mice, respectively, at the same age. The ‘high Gln’ mice also tended to have lower Glc than other WT or *Sca1*$^{154Q/2Q}$ mice at the same age, but the distinction was not as clear as for Gln, *myo*-Ins and Tau. Based on the follow-up assignments at the beginning of the study, one of these mice was scanned once, one scanned twice, one scanned three times

NIH-PA Author Manuscript

NIH-PA Author Manuscript

NIH-PA Author Manuscript

and the last one scanned four times. The abnormal neurochemical profile was observed at all scans throughout the life span of these mice. This profile was recently shown to occur in as many as 25% of the animals from the C57BL/6 background and to be associated with portosystemic shunting in the liver (Cudalbu *et al.* 2013). Since portosystemic shunting causes alterations in gene expression in many organs and an abnormal neurochemical profile in the brain, these four mice were excluded from further analysis.

Despite the lack of obvious pathological changes in the area covered by the MRS VOI, progressive neurochemical alterations in *Sca1*$^{154Q/2Q}$ mice over time were discernible even in individual animals, as demonstrated by the tCho and Tau resonances in Fig. 3. Group comparison of the neurochemical profiles demonstrated significantly lower Tau and tCho levels ($p < 0.05$) at all ages and higher Gln and tCr levels at ages 12, 24, and 39 weeks in *Sca1*$^{154Q/2Q}$ mice relative to WT controls (Fig. 4). The progressive nature of the changes in these four metabolites was apparent in their time courses (Fig. 5). In addition, the levels of NAA and Glu tended to be lower in *Sca1*$^{154Q/2Q}$ mice vs. WT mice at all ages, but this difference did not reach statistical significance (Fig. 4). None of the other neurochemicals showed significant group differences at any age either. When tCho and Tau concentrations were plotted against each other, the group separation between the *Sca1*$^{154Q/2Q}$ mice from WT controls was apparent starting at 6 weeks and became more substantial as the animals aged (Fig. 6). Consistent with the unchanged ML thickness and low scores on the severity scale, no correlations were observed between metabolite levels and histology measures.

Discussion

Using a knock-in mouse model of SCA1, we demonstrated that neurochemical alterations associated with very early effects of neurodegeneration are detectable by ultra-high field MRS. Alterations in Tau and tCho were significant starting at 6 weeks, prior to overt pathological changes in the area covered by the MRS VOI, and could be monitored in spectra from individual mice. All alterations (Tau, tCho, Gln, tCr) were progressive and, interestingly, included the earliest biochemical changes that were previously detected in a transgenic mouse model of SCA1 (Tau, Gln, tCr) (Öz *et al.* 2010b).

Pathology in transgenic vs. knock-in mouse models of SCA1

In the transgenic *SCA1*[*82Q*] line studied previously by MRS (Öz *et al.* 2010b) the pathology is restricted to the cerebellum as the transgene is only expressed in PCs. While localized to the cerebellum, the over-expression of the transgene results in severe pathology in these mice. They have significant PC dendritic attenuation and pruning that begins by 6 weeks of age and continues over the life of the animal resulting in profound dendritic atrophy, numerous heterotopic PC somata and eventual partial loss of Purkinje neurons (Clark *et al.* 1997). As a result, the *SCA1*[*82Q*] mice had received a score of 2 at 6 weeks, 3 at 12 weeks and 4 at 24 and 52 weeks on the severity scale used in this study (Öz *et al.* 2010b). While less severe, the conditional *SCA1*[*82Q*] line has a similar pathological profile (Zu *et al.* 2004) and also had received higher severity scores (Öz *et al.* 2011) than those observed in the *Sca1*$^{154Q/2Q}$ mice in this study. Note that all the histological assessment in

NIH-PA Author Manuscript

NIH-PA Author Manuscript

NIH-PA Author Manuscript

these different lines was done by the same investigator (H. Brent Clark) within the same time period in a blind fashion, enabling reliable comparisons between these different studies.

The *Sca1*$^{154Q/2Q}$ mice have a more subtle cerebellar phenotype with comparatively little atrophy of PC dendrites although some loss of PCs was noted in older animals, resulting in a severity score of 1 at end-stage. There is a reduction in the intensity of calbindin immunostaining that seems independent of marked dendritic atrophy. Despite the less severe cerebellar pathology in the *Sca1*$^{154Q/2Q}$ mice, they had a deficit in performance on the rotating rod apparatus by 5 weeks of age and ataxia by cage behavior by 20 weeks (Watase *et al.* 2002). Because the genetic abnormality is not confined to the PCs in the *Sca1*$^{154Q/2Q}$ mice, behavioral and neurochemical changes seen in these mice are likely to be influenced by the effects of the mutation on multiple types of cells, perhaps including glia.

Monitoring early neurochemical alterations in mouse models by ultra-high field MRS

The highly optimized MRS methodology utilized here ensured the reproducibility of spectral quality and pattern (Fig. 3). Of note, the cerebellum presents challenges for MRS, such as broader intrinsic line widths than other brain regions (Öz 2013), however, its anatomical landmarks present an advantage for consistent placement of the VOI within and between animals. Thus, the mean test-retest coefficient of variation using the same methodology in the mouse cerebellum is ≤ 5% for six of the reported metabolites, including tCr, tCho and Tau, and ≤ 10% for five reported metabolites, including Gln (Öz *et al.* 2010b). The high spectral quality allowed us to detect the earliest and relatively subtle neurochemical alterations starting at 6 weeks (Fig. 4), while the excellent reproducibility allowed detection of neurochemical changes in individual mice (Fig. 3).

Mice with high glutamine profile

The *Sca1*$^{154Q/2Q}$ line has not been investigated by non-invasive imaging previously. In this first MRS study of the line, we had to exclude four mice (1 WT and 3 *Sca1*$^{154Q/2Q}$) from MRS analysis in order to separate the neurochemical alterations caused by the SCA1 mutation from those associated with portosystemic shunting in mice with the C57BL/6 background. The study that recently described this phenomenon reported the abnormal high Gln profile in three other brain regions (striatum, hippocampus, and cortex) in mice (Cudalbu *et al.* 2013). Together with the current results, the portosystemic shunting appears to affect the neurochemical profile globally in the cerebrum and cerebellum. In addition to the previously reported abnormalities in Gln, *myo*-Ins and Tau, we also detected a trend for Glc in the high Gln mice, which may be a cerebellum-specific abnormality associated with portosystemic shunts. Interestingly, glucose and glycogen (the main storage form of glucose in the brain) levels in the cerebellum are higher than other brain regions (Swanson *et al.* 1989) and, together with high creatine kinase activity and tCr levels, the cerebellum appears to be distinct from other brain regions in its energy buffering capacity (Öz 2013).

In future studies with this strain, the mice can be screened by MRS at the beginning of the study and excluded as there are no other screening methods currently available for detecting the portal shunting in the liver: Portal angiography is a terminal procedure in mice. In addition, plasma ammonia and glutamine levels, as well as markers of liver function (total

NIH-PA Author Manuscript

NIH-PA Author Manuscript

NIH-PA Author Manuscript

bilirubin, aspartate amino transferase, and alanine amino transferase) are within normal limits in the high Gln mice (Cudalbu *et al.* 2013).

Neurochemical alterations in the knock-in mouse model of SCA1 in comparison to transgenic models and patients with SCA1

In the transgenic *SCA1*[*82Q*] line, the levels of tCr, Gln, and Tau were altered at 6 weeks, but converged with the levels of the control groups as the animals aged (Öz *et al.* 2010b). As such, they were the earliest biochemical changes that anticipated disease progression. Interestingly, these neurochemicals were three of the four metabolites found to be progressively different in the $Sca1^{154Q/2Q}$ mice relative to WT controls. Therefore, the neurochemical changes during the life span of the $Sca1^{154Q/2Q}$ mice appeared to reflect those that occurred in the first 6 weeks of life in the transgenic *SCA1*[*82Q*] line. Two of the three neurochemicals that marked progressive neurodegeneration, that is, significantly correlated with the histology measures, in the transgenic line, namely NAA and Glu, showed trends in the $Sca1^{154Q/2Q}$ mice. Therefore, if the cerebellar pathology in the $Sca1^{154Q/2Q}$ mice had progressed to severity scores of 2–4 before they died, we would expect that these differences in NAA and Glu would also become significant. In summary, the time courses of the neurochemical changes as they relate to the pathological progression of cerebellar disease were consistent between the two mouse lines.

Of the four neurochemicals that were significantly different in $Sca1^{154Q/2Q}$ mice relative to WT controls (tCr, Gln, tCho, and Tau), higher Gln levels than controls were also observed in the cerebellar cortex of patients with SCA1, but contrary to observations here, this difference was accompanied by lower levels of Glu (Öz *et al.* 2010a). We have also detected significantly higher tCr levels in cerebellar white matter and a trend for higher tCr in cerebellar cortex of patients with SCA1 relative to controls at a mild-moderate stage of the disease (Öz *et al.* 2010a). However, unlike tNAA, Glu and *myo*-Ins, tCr and Gln did not show strong correlations with the ataxia scores in patients (Öz *et al.* 2010a) and with the pathology scores in the transgenic SCA1 mice (Öz *et al.* 2010b, 2011), indicating that these neurochemicals mark early biochemical events in SCA1 rather than progressive disease. While we did not quantify the motor deficit in the $Sca1^{154Q/2Q}$ mice in this study, tCr and Gln may also not correlate with the behavioral phenotype in these mice based on our prior observations in humans (Öz *et al.* 2010a). Note, however, that the interpretation of behavioral studies in the $Sca1^{154Q/2Q}$ mice is complicated by the involvement of many areas of the brain and a generalized somatic wasting of the animals (Fig. 2a). Therefore, identification of the neurochemical correlates of the motor deficit in the $Sca1^{154Q/2Q}$ mice and comparisons to the ataxic phenotype in humans will require investigations of additional brain regions.

Here, we only investigated cerebellar neurochemical alterations in the $Sca1^{154Q/2Q}$ mice to enable comparisons with the transgenic line and because the cerebellar pathology is most consistently defined in these mice, facilitating VOI selection. Investigations of neurochemical changes in other brain regions and establishing the pathological and behavioral correlates of these is expected to provide further insights into the knock-in model and the neurobiology of SCA1. In particular, studying neurochemical alterations in the

NIH-PA Author Manuscript

NIH-PA Author Manuscript

NIH-PA Author Manuscript

brainstem in *Sca1*$^{154Q/2Q}$ mice is expected to be informative for comparisons with the cerebellar neurochemical alterations, as well as with alterations detected in the pons in patients (Öz *et al.* 2010a).

Implications of neurochemical changes for the neurobiology of the knock-in mouse model of SCA1

Consistent with the early neurochemical alterations we detected at 6 weeks (Tau, tCho) in the *Sca1*$^{154Q/2Q}$ mice, they develop motor incoordination at 5 weeks (Watase *et al.* 2002). On the other hand, their synaptic function in the cerebellum (between climbing fibers and PCs and between parallel fibers and PCs) is normal at 6–11 weeks (Watase *et al.* 2002), indicating that the alterations we detected in Tau, tCho, Gln, and tCr at 6 or 12 weeks reflect biochemical alterations in the presence of preserved synaptic function. While no gross pathological changes were found in PCs from 17-week-old *Sca1*$^{154Q/2Q}$ mice in a prior study also, more detailed histology revealed reduced calbindin immunofluorescence in 19-week-old *Sca1*$^{154Q/2Q}$ mice, which was interpreted as reduction in fine dendritic arbor (Watase *et al.* 2002). Therefore, the neurochemical alterations detected in this study may reflect such fine pathological changes not captured by the ML thickness or a gross pathology score.

Of the altered neurochemicals, taurine serves a number of functions in the cell, such as in osmoregulation, neuroprotection, and neuromodulation (Wu and Prentice 2010). In our prior study, taurine levels were found positively correlated with the ML thickness (Öz *et al.* 2010b). As such, decreased taurine levels were thought to indicate the thinning of the ML, consistent with the fact that somata, dendrites, and dendritic spines of PCs contain the highest taurine levels in the cerebellar cortex (Ottersen *et al.* 1988). However, in this study, taurine levels decreased without any changes in the ML thickness, indicating a purely biochemical rather than structural reason for this change.

Choline containing compounds that give rise to the tCho resonance are major constituents of the phospholipid metabolism of cell membranes and are involved in membrane synthesis and degradation, therefore disease related elevations in tCho levels are frequently associated with increased membrane turnover (Mountford *et al.* 2010). The reduced levels of tCho detected in the *Sca1*$^{154Q/2Q}$ mice may also reflect changes in phospholipid metabolism of cell membranes. Namely, disturbances in membrane phospholipid metabolism have been suggested based on post-mortem analysis of brain tissue from patients with SCA1 (Eder *et al.* 1998; Ross *et al.* 2000). On the other hand, other detectable metabolites involved in phospholipid metabolism (*myo*-Ins and PE) did not change with disease progression in the cerebella of the *Sca1*$^{154Q/2Q}$ mice.

The increase in Gln may be indicative of gliosis, as Gln is primarily localized to glial cells (Storm-Mathisen *et al.* 1992; Petroff *et al.* 1995). However, *Sca1*$^{154Q/2Q}$ mice do not display gliotic activity in the cerebellum (Watase *et al.* 2002). Hence, the Gln change may instead indicate an imbalance between the Glu and Gln pools, possibly because of a disruption of the Glu-Gln cycle, although normal synaptic function in *Sca1*$^{154Q/2Q}$ mice and unaltered Glu levels at the same ages make this interpretation also unlikely. Alternatively, the Gln

NIH-PA Author Manuscript

NIH-PA Author Manuscript

NIH-PA Author Manuscript

increase may be counterbalancing the Tau deficit as Gln also serves as an osmolyte (Miller *et al.* 2000).

Finally, the increased tCr levels may indicate abnormalities in cellular energy metabolism. Consistently, cerebellar glucose metabolism was shown to be decreased in patients with SCA1 using [^{18}F]fluorodeoxyglucose positron emission tomography (Wüllner *et al.* 2005).

Conclusions

We conclude that the *Sca1*$^{154Q/2Q}$ mice allow investigations into the earliest biochemical changes in SCA1 and that these early neurochemical alterations can be detected in SCA1 prior to overt pathology by ultra-high field MRS. These alterations are indicative of osmolytic changes and of disturbances in membrane phospholipid and energy metabolism.

Acknowledgments

We are grateful to Drs Harry Orr and Huda Zoghbi for providing the mice used in the study and for helpful discussions and comments on the manuscript. We thank Dr Cristina Cudalbu for sharing their findings on the 'high glutamine' mice prior to publication, the staff of the Center for MR Research for maintaining and supporting the NMR system, Orion Rainwater and Bob Ehlenfeldt for maintaining the mouse colonies and LuAnn Anderson for expert technical help with histology. This work was supported by the National Institute of Neurological Disorders and Stroke (NINDS) grants R21 NS060253, R01 NS070815 and the Institute for Translational Neuroscience at the University of Minnesota. The Center for MR Research is supported by National Center for Research Resources (NCRR) biotechnology research resource grant P41 RR008079, National Institute of Biomedical Imaging and Bioengineering (NIBIB) grant P41 EB015894, the Institutional Center Cores for Advanced Neuroimaging award P30 NS076408 and WM Keck Foundation.

Abbreviations used

Asc	ascorbate
CRLB	Cramér-Rao lower bounds
CSF	cerebrospinal fluid
FASTMAP	fast automatic shimming technique by mapping along projections
GABA	γ-aminobutyric acid
Glc	glucose
Gln	glutamine
Glu	glutamate
GSH	glutathione
Lac	lactate
LASER	localization by adiabatic selective refocusing
ML	molecular layer
MRS	magnetic resonance spectroscopy
***myo*-Ins**	*myo*-inositol
NAAG	*N*-acetylaspartylglutamate

NIH-PA Author Manuscript

NIH-PA Author Manuscript

NIH-PA Author Manuscript

NAA	*N*-acetylaspartate
PC	Purkinje cell
PE	phosphoethanolamine
RARE	rapid acquisition with relaxation enhancement
SCA1	spinocerebellar ataxia type 1
Tau	taurine
tCho	total choline
tCr	total creatine
TE	echo time
TR	repetition time
VAPOR	variable power radiofrequency pulses with optimized relaxation delays
VOI	volume-of-interest
WT	wild type

References

Burright EN, Clark HB, Servadio A, Matilla T, Feddersen RM, Yunis WS, Duvick LA, Zoghbi HY, Orr HT. SCA1 transgenic mice: a model for neurodegeneration caused by an expanded CAG trinucleotide repeat. Cell. 1995; 82:937–948. [PubMed: 7553854]

Clark HB, Burright EN, Yunis WS, Larson S, Wilcox C, Hartman B, Matilla A, Zoghbi HY, Orr HT. Purkinje cell expression of a mutant allele of SCA1 in transgenic mice leads to disparate effects on motor behaviors, followed by a progressive cerebellar dysfunction and histological alterations. J. Neurosci. 1997; 17:7385–7395. [PubMed: 9295384]

Cudalbu C, McLin VA, Lei H, Duarte JMN, Rougemont A-L, Oldani G, Terraz S, Toso C, Gruetter R. The C57BL/6J mouse exhibits sporadic congenital portosystemic shunts. PLoS ONE. 2013; 8:e69782. [PubMed: 23936100]

Eder K, Kish SJ, Kirchgessner M, Ross BM. Brain phospholipids and fatty acids in Friedreich's ataxia and spinocerebellar atrophy type-1. Mov. Disord. 1998; 13:813–819. [PubMed: 9756151]

Garwood M, DelaBarre L. The return of the frequency sweep: designing adiabatic pulses for contemporary NMR. J. Magn. Reson. 2001; 153:155–177. [PubMed: 11740891]

Gruetter R, Tkáč I. Field mapping without reference scan using asymmetric echo-planar techniques. Magn. Reson. Med. 2000; 43:319–323. [PubMed: 10680699]

Hennig J, Nauerth A, Friedburg H. RARE imaging: a fast imaging method for clinical MR. Magn. Reson. Med. 1986; 3:823–833. [PubMed: 3821461]

Klockgether T. Update on degenerative ataxias. Curr. Opin. Neurol. 2011; 24:339–345. [PubMed: 21734495]

Klockgether T, Paulson H. Milestones in ataxia. Mov. Disord. 2011; 26:1134–1141. [PubMed: 21626557]

Michaeli S, Garwood M, Zhu XH, DelaBarre L, Andersen P, Adriany G, Merkle H, Ugurbil K, Chen W. Proton T_2 relaxation study of water, N-acetylaspartate, and creatine in human brain using Hahn and Carr-Purcell spin echoes at 4T and 7T. Magn. Reson. Med. 2002; 47:629–633. [PubMed: 11948722]

Miller TJ, Hanson RD, Yancey PH. Developmental changes in organic osmolytes in prenatal and postnatal rat tissues. Comp. Biochem. Physiol., Part A Mol. Integr. Physiol. 2000; 125:45–56.

NIH-PA Author Manuscript

NIH-PA Author Manuscript

NIH-PA Author Manuscript

Mountford CE, Stanwell P, Lin A, Ramadan S, Ross B. Neurospectroscopy: the past, present and future. Chem. Rev. 2010; 110:3060–3086. [PubMed: 20387805]

Ottersen OP, Madsen S, Storm-Mathisen J, Somogyi P, Scopsi L, Larsson LI. Immunocytochemical evidence suggests that taurine is colocalized with GABA in the Purkinje cell terminals, but that the stellate cell terminals predominantly contain GABA: a light- and electronmicroscopic study of the rat cerebellum. Exp. Brain Res. 1988; 72:407–416. [PubMed: 3066636]

Öz, G. Manto, M.; Gruol, DL.; Schmahmann, JD.; Koibuchi, N.; Rossi, F.; Rossi, F. Handbook of the Cerebellum and Cerebellar Disorders. Vol. Vol. 1. Netherlands: Springer Dordrecht; 2013. MR Spectroscopy in Health and Disease; p. 713-733.

Öz G, Hutter D, Tkáč I, Clark HB, Gross MD, Jiang H, Eberly LE, Bushara KO, Gomez CM. Neurochemical alterations in spinocerebellar ataxia type 1 and their correlations with clinical status. Mov. Disord. 2010a; 25:1253–1261. [PubMed: 20310029]

Öz G, Nelson CD, Koski DM, et al. Noninvasive detection of presymptomatic and progressive neurodegeneration in a mouse model of spinocerebellar ataxia type 1. J. Neurosci. 2010b; 30:3831–3838. [PubMed: 20220018]

Öz G, Vollmers ML, Nelson CD, Shanley R, Eberly LE, Orr HT, Clark HB. In vivo monitoring of recovery from neurodegeneration in conditional transgenic SCA1 mice. Exp. Neurol. 2011; 232:290–298. [PubMed: 21963649]

Petroff OA, Pleban LA, Spencer DD. Symbiosis between in vivo and in vitro NMR spectroscopy: the creatine, N-acetylaspartate, glutamate, and GABA content of the epileptic human brain. Magn. Reson. Imaging. 1995; 13:1197–1211. [PubMed: 8750337]

Provencher SW. Estimation of metabolite concentrations from localized in vivo proton NMR spectra. Magn. Reson. Med. 1993; 30:672–679. [PubMed: 8139448]

Provencher SW. LCModel & LCMgui User's Manual. 2001

Ross BM, Eder K, Moszczynska A, et al. Abnormal activity of membrane phospholipid synthetic enzymes in the brain of patients with Friedreich's ataxia and spinocerebellar atrophy type-1. Mov. Disord. 2000; 15:294–300. [PubMed: 10752579]

Schöls L, Bauer P, Schmidt T, Schulte T, Riess O. Autosomal dominant cerebellar ataxias: clinical features, genetics, and pathogenesis. Lancet Neurol. 2004; 3:291–304. [PubMed: 15099544]

Storm-Mathisen J, Danbolt NC, Rothe F, Torp R, Zhang N, Aas JE, Kanner BI, Langmoen I, Ottersen OP. Ultrastructural immunocytochemical observations on the localization, metabolism and transport of glutamate in normal and ischemic brain tissue. Prog. Brain Res. 1992; 94:225–241. [PubMed: 1363142]

Swanson RA, Sagar SM, Sharp FR. Regional brain glycogen stores and metabolism during complete global ischaemia. Neurol. Res. 1989; 11:24–28. [PubMed: 2565546]

Tkáč, I.; Zacharoff, L.; Dubinsky, JM. Longitudinal study of neurochemical changes in Q140 mouse model of Huntington's disease. Nineteenth Scientific Meeting of the ISMRM; Montreal, Canada. 2011. p. 2288

Watase K, Weeber EJ, Xu B, et al. A long CAG repeat in the mouse Sca1 locus replicates SCA1 features and reveals the impact of protein solubility on selective neurodegeneration. Neuron. 2002; 34:905–919. [PubMed: 12086639]

Wu JY, Prentice H. Role of taurine in the central nervous system. J. Biomed. Sci. 2010; 17(Suppl 1):S1. [PubMed: 20804583]

Wüllner U, Reimold M, Abele M, Burk K, Minnerop M, Dohmen BM, Machulla HJ, Bares R, Klockgether T. Dopamine transporter positron emission tomography in spinocerebellar ataxias type 1, 2, 3, and 6. Arch. Neurol. 2005; 62:1280–1285. [PubMed: 16087769]

Xin L, Gambarota G, Mlynárik V, Gruetter R. Proton T_2 relaxation time of J-coupled cerebral metabolites in rat brain at 9.4 T. NMR Biomed. 2008; 21:396–401. [PubMed: 17907262]

Zoghbi HY, Orr HT. Glutamine repeats and neurodegeneration. Annu. Rev. Neurosci. 2000; 23:217–247. [PubMed: 10845064]

Zu T, Duvick LA, Kaytor MD, Berlinger MS, Zoghbi HY, Clark HB, Orr HT. Recovery from polyglutamine-induced neurodegeneration in conditional SCA1 transgenic mice. J. Neurosci. 2004; 24:8853–8861. [PubMed: 15470152]

NIH-PA Author Manuscript

NIH-PA Author Manuscript

NIH-PA Author Manuscript

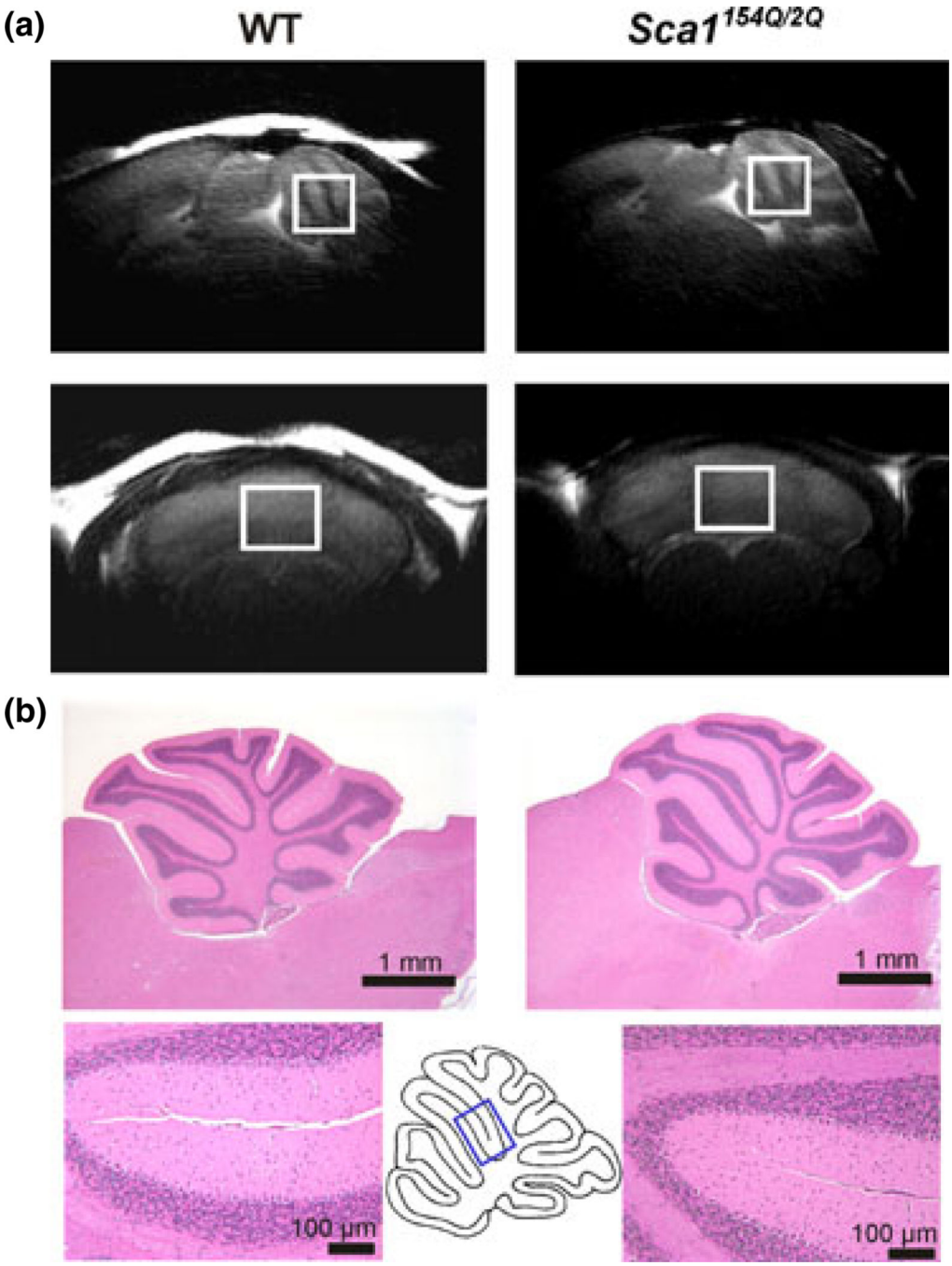

Fig. 1.

(a) Mid-sagittal (top row) and coronal (bottom row) T_2-weighted images showing the placement of the cerebellar volume-of-interest in a *Sca1*$^{154Q/2Q}$ mouse (right) and a wild-type mouse (left) at 39 weeks. (b) Histological assessment in a *Sca1*$^{154Q/2Q}$ mouse (right) and a wild-type mouse (left) at 39 weeks. The top slides show the entire cerebellum, the bottom slides show an area indicated on the mid-sagittal cerebellum scheme. Slides were stained with hematoxylin-and-eosin and the bars indicate dimensions, 1 mm or 100 μm.

NIH-PA Author Manuscript
NIH-PA Author Manuscript
NIH-PA Author Manuscript

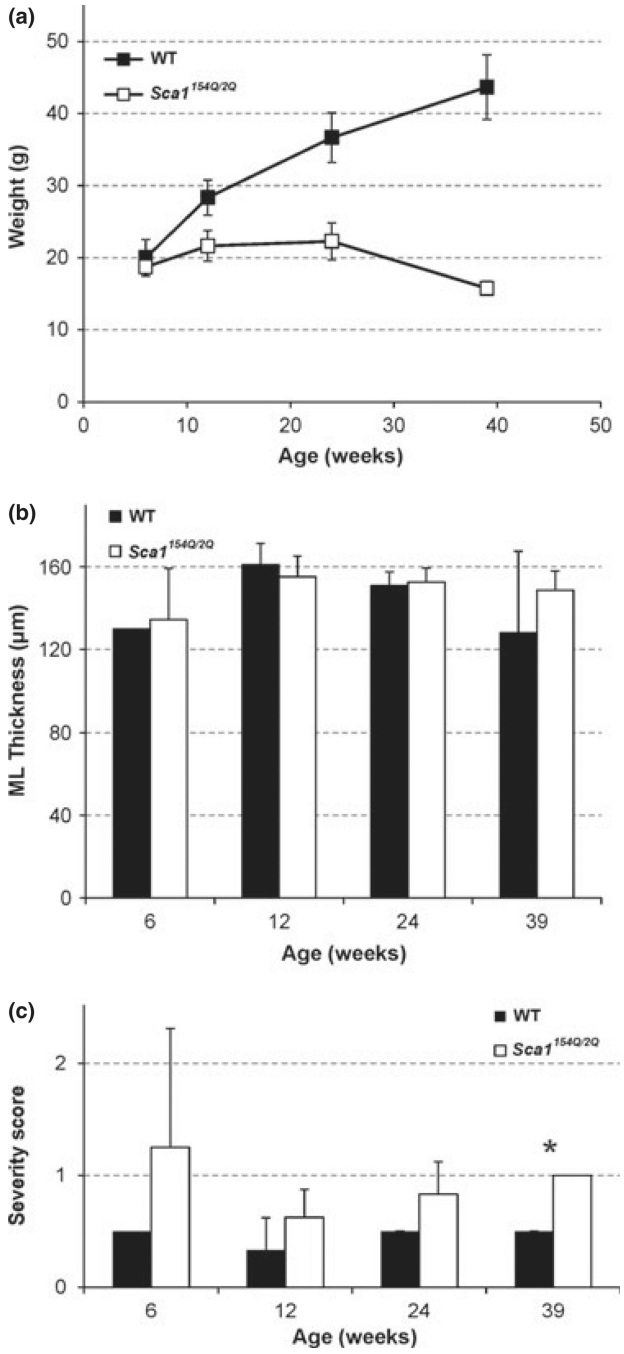

Fig. 2.

Mean (a) weights, (b) molecular layer thickness in the primary fissure and (c) global pathological severity scores of the *Sca1*$^{154Q/2Q}$ and wild-type mice at 6, 12, 24, and 39 weeks of age. Error bars indicate standard deviations. * indicates $p < 0.05$.

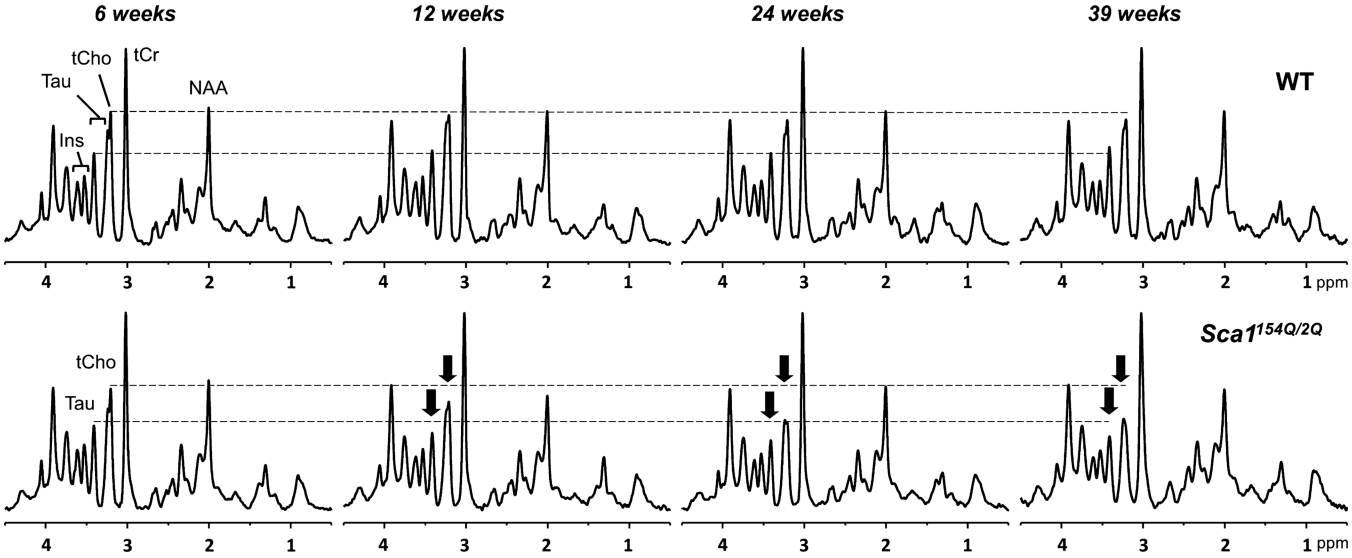

Fig. 3.

Localized proton MR spectra [localization by adiabatic selective refocusing (LASER), TE = 15 ms, TR = 5 s] obtained from one wild-type (upper row) and one *Sca1*$^{154Q/2Q}$ mouse (lower row) across their life spans. The spectra were processed identically, weighted with the same Gaussian function prior to Fourier transformation and scaled based on neurochemical concentrations obtained by LCModel. The longitudinal alterations in total choline and taurine in the spectra of the *Sca1*$^{154Q/2Q}$ mouse are shown with arrows.

NIH-PA Author Manuscript NIH-PA Author Manuscript NIH-PA Author Manuscript

NIH-PA Author Manuscript
NIH-PA Author Manuscript
NIH-PA Author Manuscript

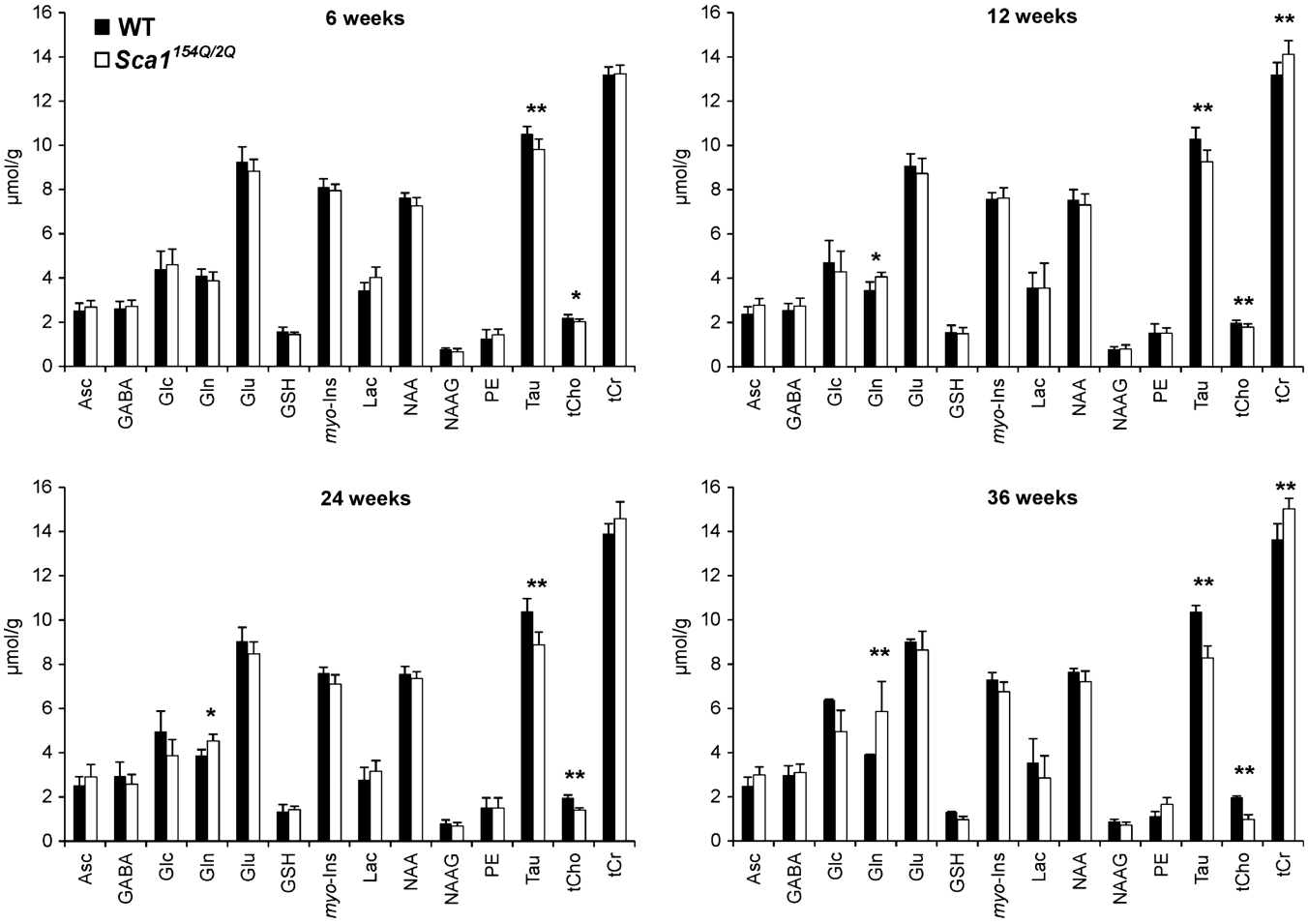

Fig. 4.

Cerebellar neurochemical profiles of the *Sca1*$^{154Q/2Q}$ (white bars) and wild-type (black bars) mice at four ages. Error bars indicate standard deviations. * indicates $p \leq 0.05$, ** indicates $p \leq 0.01$.

NIH-PA Author Manuscript
NIH-PA Author Manuscript
NIH-PA Author Manuscript

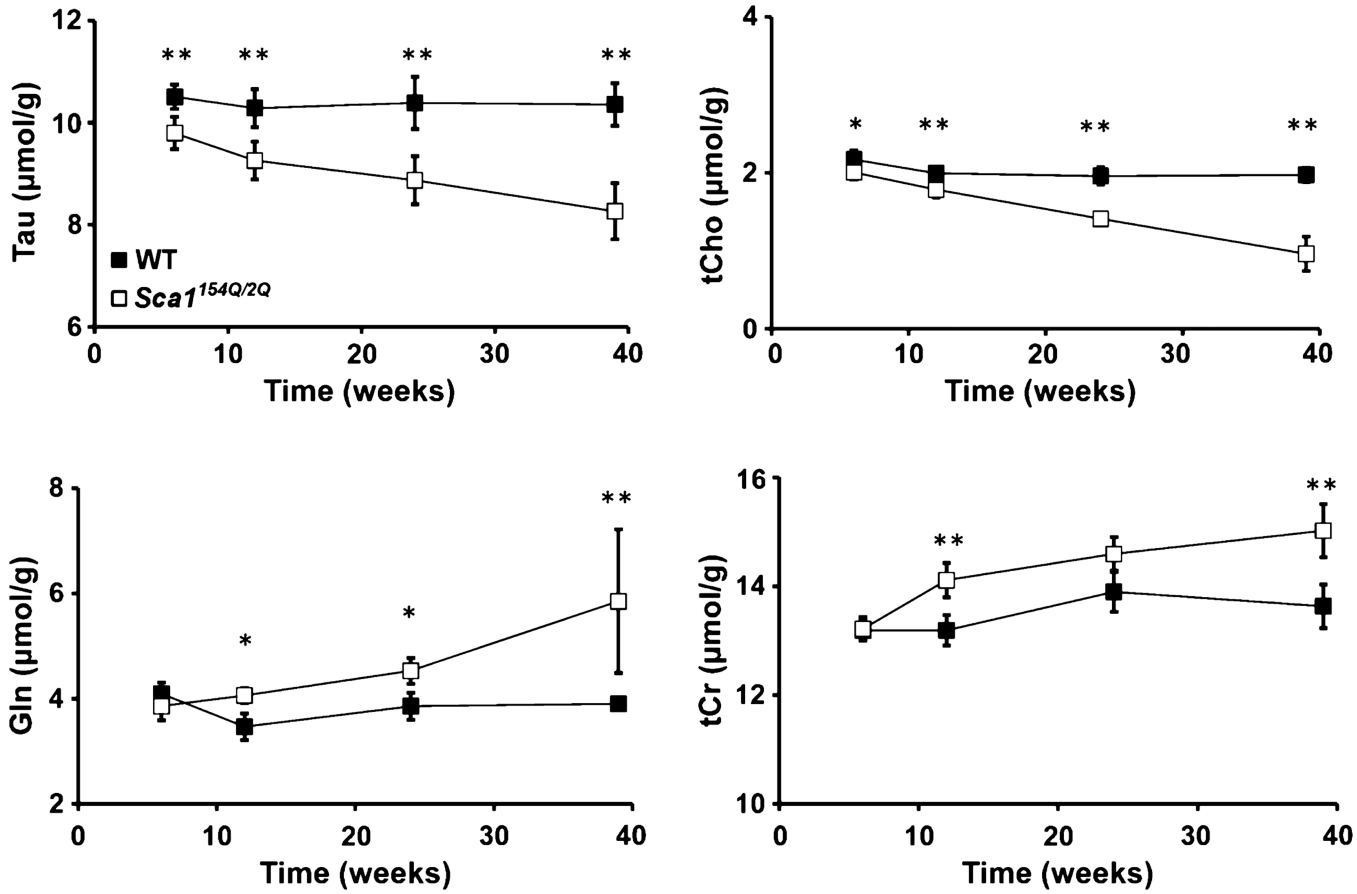

Fig. 5.

Time courses of taurine, total choline, glutamine, and total creatine in the cerebella of the *Sca1*$^{154Q/2Q}$ (white squares) and wild-type (black squares) mice. Error bars indicate standard deviations. * indicates $p \leq 0.05$, ** indicates $p \leq 0.01$.

NIH-PA Author Manuscript
NIH-PA Author Manuscript
NIH-PA Author Manuscript

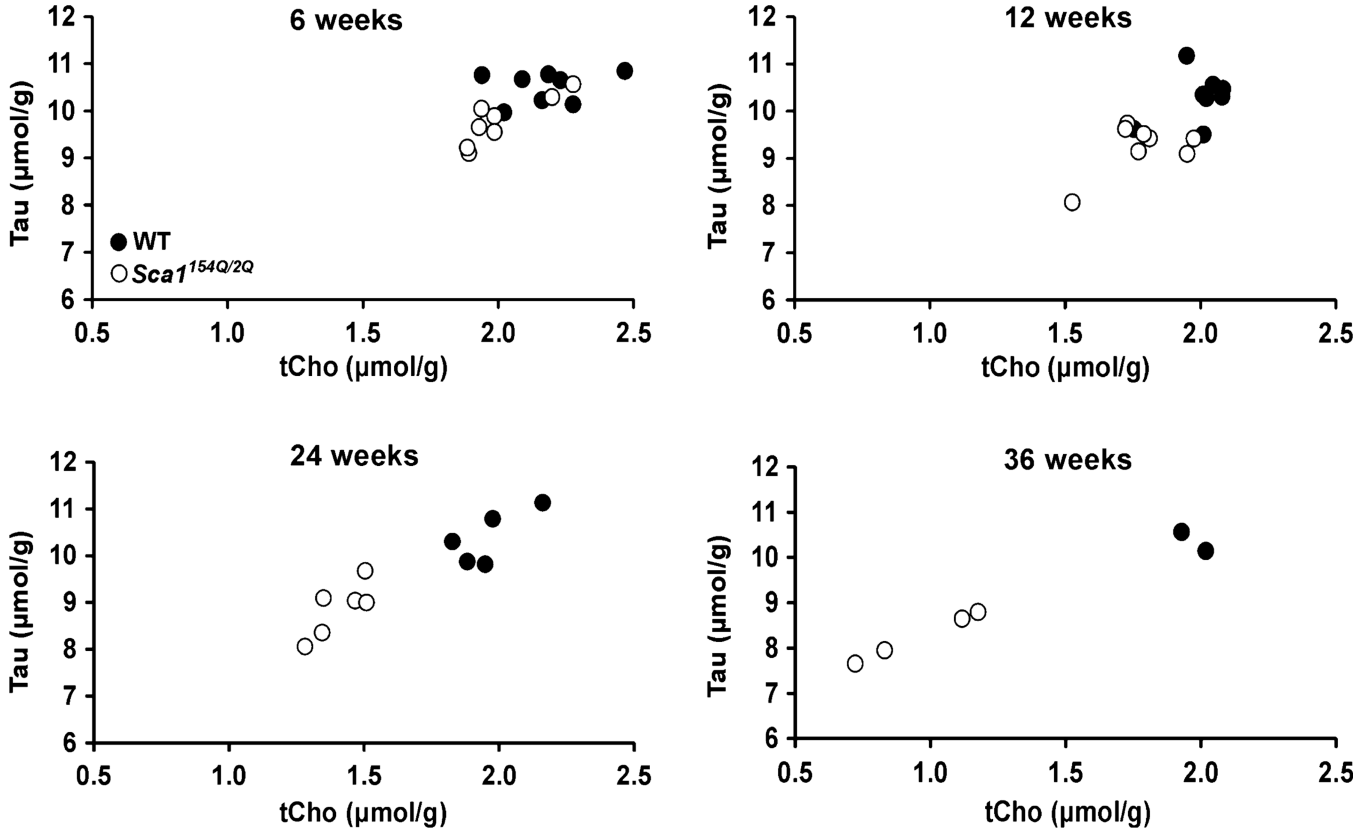

Fig. 6.

Separation of *Sca1*$^{154Q/2Q}$ (white circles) from wild-type mice (black circles) at each age. Concentrations of taurine and total choline obtained from the cerebella of individual mice are plotted.